Research Article

Performance of Ladle Furnace Slag in Mortar under Standard and Accelerated Curing

Iffat Sultana (ID) **and G. M. Sadiqul Islam** (ID)

Department of Civil Engineering, Chittagong University of Engineering & Technology, CUET, Chattogram 4349, Bangladesh

Correspondence should be addressed to G. M. Sadiqul Islam; gmsislam@cuet.ac.bd

This research preliminarily investigated the suitability of a locally available ladle furnace slag (LFS) as a partial replacement of cement in mortar. The raw material was first characterized to obtain its chemical and physical properties through particle size distribution, X-ray fluorescence (XRF), X-ray diffraction (XRD), and scanning electron microscopy (SEM). Later, the raw LFS was classified into two categories: (i) raw LFS and (ii) sieved (passing through #200 sieve) LFS and incorporated in mortars as a partial replacement of cement. Mortar prisms with 5, 10, 15, 20, 25, and 50% LFS (raw and sieved) were prepared and cured under normal temperature (NTC) for 7, 28, and 56 days. Additional mortar prisms (with raw and sieved LFS) were prepared by curing them under high-temperature accelerated curing (HTAC) for 7 days. The characterization tests suggest that CaO, SiO_2, MgO, and Al_2O_3 are the main compounds of raw LFS used in this study. The mineralogical phases present in the raw slag are calcio-olivine, akermanite, α-quartz, merwinite, magnetite (Fe_3O_4), and calcium-aluminium oxide. Both raw and sieved LFS-blended mortars yield good consistency up to 25% cement replacement in mortars. The compressive strength of NTC mortar suggests that 5% and 10% replacement of cement with raw and sieved LFS yields higher strength than the control mortar. Seven days strengths of raw and sieved LFS blended mortars obtained for HTAC are closely comparable to that of 28 days under NTC. This study recommends that LFS could be a sustainable supplementary material to use as a partial replacement of cement in mortar, preferably up to a level of 15% for standard works.

1. Introduction

Concrete, the second most utilized material on Earth (after water), creates environmental issues, arising mainly from its constituent materials. For example, excessive use of natural sand and aggregates creates environmental instability; use of drinking water abundantly is an issue since it causes gradual lowering of the groundwater table. The production and use of cement, a critical component of concrete, is proven to impact the environment negatively. Studies report that 8% of the global greenhouse gas (GHG) emission is due to the production of cement [1].

Globally, cement production has been reduced or kept checked in the last decade due to the negative impact on the environment [2]. In contrast, Bangladesh has seen an increase in cement production by 10–12% in the past decade

[3]. An increase in cement production means an increase in cement use, consequently increasing the negative impacts on environment. It is essential to reduce the use of cement as much as possible to curb the environmental pollution. This could be achieved by diverging towards sustainable concrete production incorporating supplementary cementitious materials (SCM) and/or supplementary filler materials (SFM) and/or recycled water and reducing the dependency on drinking water [4].

Various studies report effective alternative use of different types of solid wastes, e.g., waste clay brick, ceramic waste powder, and glass powder [5, 6]. Pozzolanic and cementitious properties are available in industrial by-products, e.g., ground granulated blast furnace slag (GGBS), silica fume, steel slag, cement kiln dust [7–11]; ashes, e.g., fly ash [12], rice husk ash (RHA) [13], sugarcane bagasse ash

[14], coconut ash [15], wood fibre ash and corn fibre ash [16]; and ceramic wastes [17]. These materials can be used either directly (as-received raw materials) or after being chemically treated (with an activator or reagent to improve their properties as SCM).

In Bangladesh, several studies considered SCM [18–20] for mortars and concrete. Mainly, fly ash and RHA have been the point of interest to the researchers. Steel slags, available in plenty, primarily due to the growing industries (∼400 steel mills), have also been considered for a smaller number of studies [21]. Approximately, 1.1–1.3 million metric tonnes of steel slag are produced per annum in Bangladesh [21]. These include ladle furnace slag (LFS)—a secondary by-product of the steel making process. LFS in general is generated in the second stage of the steel manufacturing process resulting in a lesser production compared with the primary slags, e.g., basic oxygen furnace slag (BOFS) and electric arc furnace slag (EAFS). Nevertheless, considering a LFS generation of 0.3–0.7% of the steel production, the annual production (30 million tonnes) of LFS worldwide is quite significant [22]. Previously, the steel industry in Bangladesh used to dump this LFS into open lands just as waste. In recent times, several alternative (other than SCM) uses of this by-product have been identified by the researchers: (i) brick production with other steel slags; (ii) filtering bed material; (iii) in the rotatory furnace of Portland clinker; and (iv) agricultural fertilizer. However, the application is still limited [23, 24].

The applicability of LFS as SCM has been investigated in mortars, concrete pavement work [24], and self-compacting concrete [25]; mortar for rigid and flexible concrete [26]; soil improvement [27]; stabilizing embankment soil [28]; filler material in asphalt mix [29]; and strengthening clay soil [11].

On the properties of LFS as SCM, a database is available globally [8, 24, 28, 30–33]. Previous studies report that LFS contains calcium oxide (CaO), silicon dioxide (SiO_2), aluminium oxide (Al_2O_3), and magnesium oxide (MgO) on many occasions. Kriskova et al. [34] report that the concentration of these materials is 92.3% and Shi and Hu [35] report that it is 92.2% in total. The overall presence of primary constituents varies from 88% to 94% [36–38]. The ladle finally refines steel by removing these oxides as waste form inside the ladle slag.

The morphology of LFS particles, in general, is found to have rough surfaces with local crystalline growth, dusty materials, and greyish white powder-like appearance [24, 26, 39, 29] (Figure 1). Shi [31] reports that LFS alone may not induce reasonable cementitious properties in a mortar, but LFS-GGBS blended cement paste with an activator (e.g., sodium silicate, Na_2SiO_3) can produce good quality mortar [24]. Manso et al. [32] report that if LFS is used as a substitution of binder and fine aggregates, it may produce mortars of standard quality. Shi and Hu [35] blended LFS with silica flour and fly ash, and then cured under autoclave (∼175°C) to induce good cementitious properties.

A recently published review article [40] on LFS has incorporated substantial amount of study reports. This and other studies indicate that LFS has the potential to be a partial cement supplement, but its physical and mineral properties vary broadly and are dependent on the geography and industrial processes [40]. Therefore, local LFS products need proper investigation before being considered for application in construction, especially when the manufacturing process is unique, for example, in the steel mills of Bangladesh, no BOFS is produced and LFS is generated only in the ladle refining furnace (LRF). As such, this study focused on the assessment of LFS as a partial replacement of cement.

This study reports the results of mechanical properties of raw and sieved (through #200 sieve) LFS blended mortars following the characterization of the raw LFS powder. The characterization results include chemical, physical, mineralogical, and morphological properties of raw LFS, identified through sophisticated testing facilities and compared with standard cement samples, i.e., CEM-I. The mechanical properties of raw and sieved LFS blended mortars are investigated under normal temperature curing (NTC) and compared with the control samples. Additionally, mechanical properties of LFS blended mortars under high-temperature accelerated curing (HTAC) are investigated to quantify the effect of temperature on strength gain/loss.

2. Materials

2.1. Regular Mortar Materials. Cement (CEM-I) was used as the reference material. As per EN-197, its strength class is 42.5N. The key properties of CEM-I: normal consistency = 25%, soundness by Le Chatelier's test = 4.5 mm, specific gravity = 3.12, clinker = 95–100%, and gypsum = 0–5%. For preparing mortars, EN standard sand was used. This (reference) sand is a natural siliceous material composed of rounded particles and has a silica content of at least 98%. The moisture content was less than 2%, represented by the mass of the dry sample as a percentage. Tap water was used for preparing mortar prisms.

2.2. Supplementary Material Used to Replace Cement. Ladle furnace slag (LFS) was used as the prospective supplementary cementitious material (SCM). The material was collected from a renowned local Steel Re-Rolling Mill of Bangladesh. An impression of just produced LFS from the furnace is shown in Figure 2. Two types of LFS samples were used. The as-received LFS powder is termed as 'raw LFS' and the one sieved through a #200 sieve is termed as 'sieved LFS' (see Figure 3). The use of a finer LFS sample allowed to investigate the effect of fineness since the fineness of steel slag can play a role in improving the fresh and hardened properties of mortar [41, 42].

3. Experimental Program

3.1. Characterization Tests of LFS and CEM-I. X-ray fluorescence (XRF) spectroscopy was used to characterize and identify the elements in CEM-I and raw LFS powders. The method uses a primary incident X-ray on a sample that allows the sample to emit secondary rays called–fluorescent. The fluorescent rays are unique for a specific element in a material, thus allowing characterization and identification of

(a)   (b)   (c)
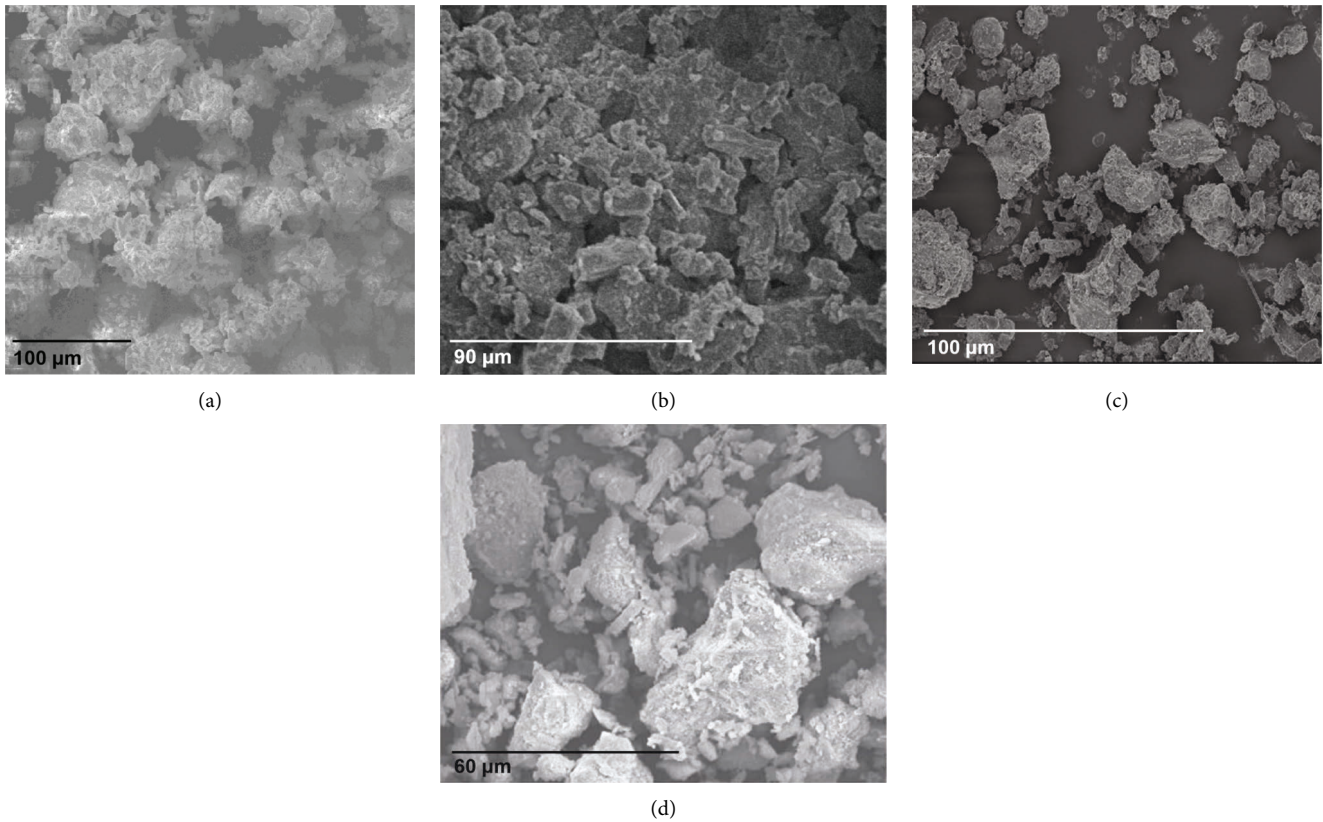

(d)

FIGURE 1: SEM images of LFS: (a) [24]; (b) [26]; (c) [39]; (d) [29].

FIGURE 2: LFS as produced in Mirsarai plant of BSRM.

elements in a sample. Details of XRF method can be found in Irshidat and Al-Nuaimi [43], and Rodriguez et al. [44].

The crystalline phases or compounds of CEM-I and raw LFS were identified using X-ray diffraction (XRD) technique. X-ray diffractometer with monochromatic CuKα source and curved graphite, and single-crystal chromator (40 kV, 30 mA) was used. Samples were firmly compacted on the reverse side of the specimen holder, against a glass slide. Each sample was analysed (for potential diffraction paths of the lattice) over a 2θ range of 3°–60° at a scan rate of 1° per minute with an increment of

0.1°. More details can be read from Meier et al. [45] and De Villiers and Lu [46]. Figure 4 illustrates XRD method (adapted from [46]).

The morphology and topography (size and shape and surface texture) of the particles of CEM-I and raw LFS were assessed from the microscopic images using scanning electron microscopy (SEM) technique with an accelerating voltage of 15 kV. SEM can visualize the surface of a particle with high to ultra-high-resolution images of a particle in a sample with its crystallography composition [47].

(a)   (b)

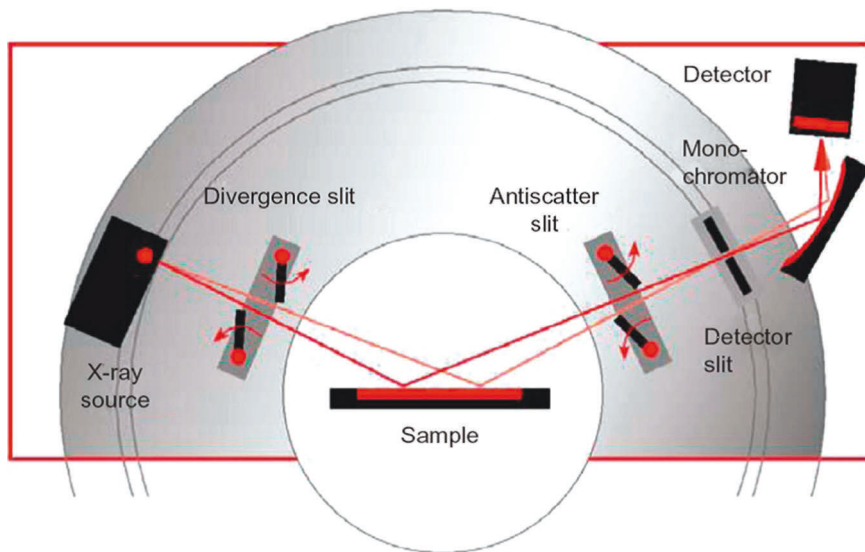FIGURE 3: Powdered ladle furnace slag (LFS) used in this study (a) raw LFS powder; (b) sieved (#200) LFS powder.

FIGURE 4: The Bragg–Brentano geometry used in modern diffractometers [46].

3.2. Mortar Constituents and Compositions. A total of 15 control mortar prisms was prepared with cement, sand, and water. A total of 132 (includes 3 replicates) LFS blended mortar prisms were prepared with cement, LFS (66 with raw and 66 with sieved), sand, and water. The mixing ratio was 1 : 3 : 0.5 (binder: sand: water) according to EN 196-1. Cement in the mortar was partially replaced by 5, 10, 15, 20, 25, and 50% LFS (both for raw and sieved, separately) by weight. An additional 36 mortar prisms (with raw and sieved LFS) were prepared for HTAC tests. The detailed mix compositions and sample names of mortars are given in Table 1.

3.3. Flow of Mortar. Required amount of materials for mortar was mixed in a mechanical mixer machine as per EN 196-1. The mixer machine was comprised of a stainless-steel bowl (capacity ~5 litres) and blades. The bowl was placed in such way that it was firmly attached to the mixer frame during mixing. The blade rotated about its axis, powered by an electric motor in planetary motion around the axis of the bowl. The speeds of the blade were controlled automatically.

The flow of hydraulic cement mortar was determined using the flow table in compliance with ASTM C1437. The

test specimen was moulded on a 250 mm diameter table ASTM C230. A conical frustum shape mould with a bottom diameter of 100 mm and a top diameter of 70 mm was used. Once filled with mortar paste, the mould was removed, leaving the mortar on the table, and the table was cyclically lowered and raised 25 times (within 15 seconds). After that, the flow, i.e., the increase in the average diameter of the fresh specimen was measured. Flow value was calculated after dividing the increased diameter by the original diameter and reported as a percentage. Flow value for each type of sample was tested for three times in order to obtain mean value.

3.4. Compressive Strength of Mortar. Mortars for strength tests were prepared as mentioned above. The sample with plastic consistency from the mixer machine was poured inside a 3-gang steel mould of $40 \times 40 \times 160$ mm internal dimensions. The mortars were compacted using a regular jolting method inside the mould. The specimens were kept in the mould for about 24 h in a humid environment and then demoulded. As mentioned earlier, 108 mortar prisms with 5–50% cement replacement were prepared using raw and sieved LFS for different curing periods (7, 28, and 56 days).

TABLE 1: Mix composition of mortars for a single mix in a mixer machine as adopted in this study.

Sl	Sample name	Cement (gm)	LFS (gm)	Sand (gm)	Water (gm)
1	ML0 = control (no LFS)	450	—		
2	ML5R = 5% raw LFS	427.5	22.5		
3	ML10R = 10% raw LFS	405	45		
4	ML15R = 15% raw LFS	382.5	67.5		
5	ML20R = 20% raw LFS	360	90		
6	ML25R = 25% raw LFS	337.5	112.5		
7	ML50R = 50% raw LFS	225	225	1350	225
8	ML5S = 5% sieved LFS	427.5	22.5		
9	ML10S = 10% sieved LFS	405	45		
10	ML15S = 15% sieved LFS	382.5	67.5		
11	ML20S = 20% sieved LFS	360	90		
12	ML25S = 25% sieved LFS	337.5	112.5		
13	ML50S = 50% sieved LFS	225	225		

The mortar prisms were then cured under normal water until the compressive strength was tested.

Few samples (30 in total; including control) were prepared for longer age curing (90 and 180 days) with selected blends, viz. 0, 25, and 50% LFS (only three different percentages were considered due to restricted time and budget). Curing time significantly affects mortar properties as the hydration of cement depends on the availability of sufficient water. Proper curing also helps fill the micropores in the hydrated cement paste, thereby increasing the density of mortar. The microstructural improvement contributes to the strength development of the cement paste matrix [48].

The compressive strengths of all cured mortar specimens were measured using a jig inside the standard (EN 196-1) compression testing machine. The jig could hold the mortar prism in such a way that the square area (40 × 40 mm) was set under the loading plate. The resultant of the forces passed through the centre of the specimen.

3.5. Mortar with High-Temperature Accelerated Curing (HTAC).

To investigate the effect of high-temperature curing, i.e., accelerated curing, additional mortar samples were prepared following the guidelines set in BS 3892 (1982). A total of 18 prisms with raw LFS and 18 with sieved LFS were cast which included 3 replicates of each type, i.e., 5, 10, 15, 20, 25, and 50% of LFS. Prepared samples were demoulded after 24 hours and then kept in a water bath for standard temperature curing (20±1°C) for 4 days. After that, the samples were transferred to another water bath for high-temperature curing at 50±1°C for 46 hours (Figure 5) and then shifted to a standard temperature regime. After 2 hours of standard curing (20±1°C), essentially producing samples of 7 days curing, the mortar specimens were taken for compressive strength testing.
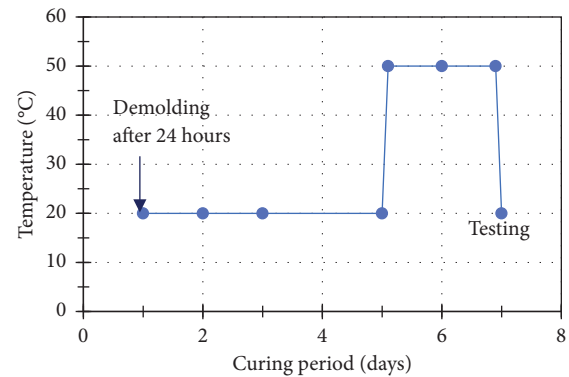

FIGURE 5: Temperature variation with time for HTAC samples.
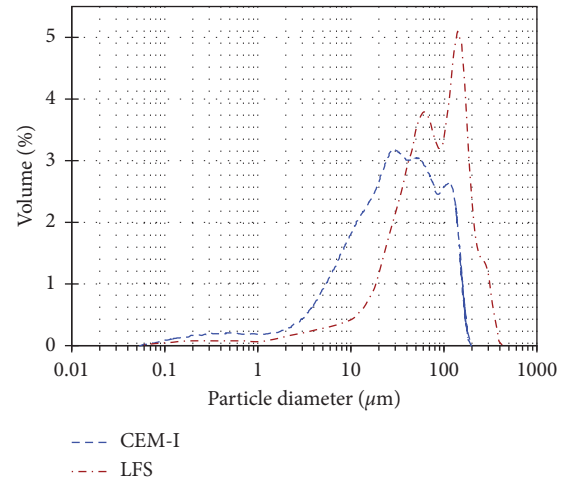
FIGURE 6: Particle size distribution of CEM-I and raw LFS.

4. Test Results and Discussion

4.1. Particle Size Distribution (PSD).

Particle size distributions of CEM-I and raw LFS are shown in Figure 6. Approximately, 90% of the CEM-I particles are smaller than 107 μm in size, and 10% are smaller than 4.28 μm. The mean and median particle sizes of CEM-I are 22.8 μm and 29.2 μm, respectively. For raw LFS, 90% of the particles are smaller than 188 μm, and 10% are smaller than 16.0 μm. The mean and median particle sizes of raw LFS are 59.2 μm and 73.7 μm, respectively. The SEM test results also indicate that raw LFS comprises coarser-sized particles than CEM-I [49]. Therefore, the material was sieved using a 75 μm sieve to get the finer part as the size of the particles plays a vital role in

the reactions in cementitious media and influences hardened mortar properties [41, 50]. PSD for sieved was not determined in this study.

In general, raw LFS used in this study has larger sized particles compared with the previous studies. For example, Türker et al. [51] reported that 92% of the raw LFS particles were smaller than 30 μm, and Salman et al. [52] reported that 80% of the raw LFS particles were smaller than 59 μm. Salman et al. [52] also found that d50 of raw LFS is 35.7 μm. Researchers studied the suitability of LFS processed to finer particle size, e.g., d50 = 10~28 μm [33, 39]. This study also considered sieving of raw materials to bring them to a size finer than 75 μm and compared the performance of both raw and sieved LFS as SCM.

4.2. Chemical Composition of Test Materials.

The chemical compositions of CEM-I and LFS are given in Table 2. The main compounds found are CaO, SiO_2, MgO, and Al_2O_3, representing more than 92% of the total mass. A study found CaO, SiO_2, MgO, and FeO (low percentage) as the main chemical compositions and comprised about 88–92% of the total mass of LFS [53]. Other studies (e.g., [8, 54]) suggest that CaO, SiO_2, MgO, and Al_2O_3 are present in LFS (see Table 2), which is common for any carbon and steel production slags [40]. These oxides were mentioned as inevitable constituents of silicates and aluminates of calcium and magnesium found in LFS [26].

4.3. Mineralogical Composition of Test Materials.

The crystalline compositions of CEM-I and raw LFS are shown in Figures 7(a) and 7(b), respectively. Table 3 illustrates the denotation and chemical formula of the phases present in both CEM-I and LFS. Dominant hump of diffraction was noticed in between $2\theta = 29°$ and $35°$ in the case of CEM-I. The mineralogical phases detected in CEM-I are Alite (C3S), larnite, i.e., calcium silicate (Ca_2SiO_4) in polymorph states, e.g., β-Ca_2SiO_4, Aluminate (C3A), Brownmillerite (C4AF) and Periclase (MgO). Higher amount of CaO content has the contribution in developing C-S-H gel. Besides, the reaction between CaO and CO_2 is the cause of forming calcite [49].

The mineralogical compounds detected in LFS could be attributed to calcio-olivine (Ca_2SiO_4), akermanite ($Ca_2Mg(Si_2O_7)$, α-quartz (SiO_2), merwinite ($Ca_3MgSi_2O_8$), magnetite (Fe_3O_4), and calcium-aluminium oxide ($CaAl_2O_4$). Important changes in the peak were observed in the range of $2\theta = 27°$ and $33°$. The results of the XRD analysis of the investigated LFS are also comparable with the results reported in a previous study [49]. Calcium and silicates under various allotropic forms were the major compounds available in LFS. Calcium-aluminium oxide present in LFS helps to form $CaCO_3$ and C-S-H gel. Besides, unreacted slag fills the pores and voids which has an effect in densifying the matrix, thus the strength increased [55].

4.4. Morphological Properties Obtained by SEM.

Figures 8(a) and 8(b) give SEM micrographs of CEM-I and LFS, respectively. CEM-I is mainly composed of clinker (95%). SEM image shows relatively smooth and angular surfaces of the grinded clinker. LFS is found with a dusty product on its surface. The surface morphology of LFS particles indicates rough-edged surfaces. A significant number of surface cracks are also noticed. The cracks occur mainly on the periphery of the grains and are parallel to the edges of the grains. Radenović et al. [54]; Natali Murri et al. [39], and Skaf et al. [29] also found similar topography and shape of LFS particles in their studies. The particle size distribution analysis described earlier is also well matched with this SEM data.

4.5. Flow Value of Mortar.

Mortar pastes prepared with cement and various levels of both raw and sieved LFS were tested for workability. The workability of raw and sieved LFS blended mortars are compared with that of the control mortar in Figure 9. The flow value of the control cement mortar was found to be 105%. In general, the flow value of LFS blended mortar decreases with the increase in SCM as cement replacement. The flow variation was 14–23% in the case of raw LFS replacement. When the cement is replaced with 5–25% sieved LFS, it varies from 2 to 19%. Reasonably good consistency mortar was produced for up to 20% LFS replacement. According to Balakrishnan et al. [56] and McCarthy et al. [57], flow values of masonry mortar with 10–50% cement replacement with fly ash did not exceed 30% relative to the control mortar. Santamaria et al. [58] reported that SCM of polyhedral crystals creates an inwards capillary action to fill the hollow spaces when water comes into contact. According to the PSD curve (Figure 5), the mean size of raw LFS is higher than cement. As a result, with higher cement replacement, the free space between particles increases, affecting their external capillarity. This may lead to the increase-decrease-increase pattern of flow values. As shown in the figure, mortar with sieved LFS shows better workability compared with the raw LFS as it acts as a filler. Compared with cement, sieved LFS possesses a high specific area and the voids between cements are filled with sieved LFS, increasing the particle contact. Even though both particles absorb water, due to external capillarity, higher water absorption is noticed. Therefore, it is concluded that a higher presence of fines (50% replacement) demanded increased water. An earlier study by Zykova et al. [59] concluded that the composition with complex filler fractions has the highest water absorption.

4.6. Compressive Strength of Mortar

4.6.1. Influence of LFS Size.

Figures 10(a) (for raw LFS) and 10(b) (for sieved LFS) present the compressive strength of mortar as a function of LFS replacement levels (7, 28, and 56 days curing under standard temperature, i.e., 20±1°C). In general, sieved LFS provides better strength performance than raw LFS. The trend follows earlier study with fly ash [60] which reports that smaller particles have higher reactivity in cementitious media. Similar better performance with finer LFS was reported by Shi and Hu [35]. On the other hand, when the total cementing material content was

TABLE 2: Chemical composition of CEM-I and raw LFS used in this study.

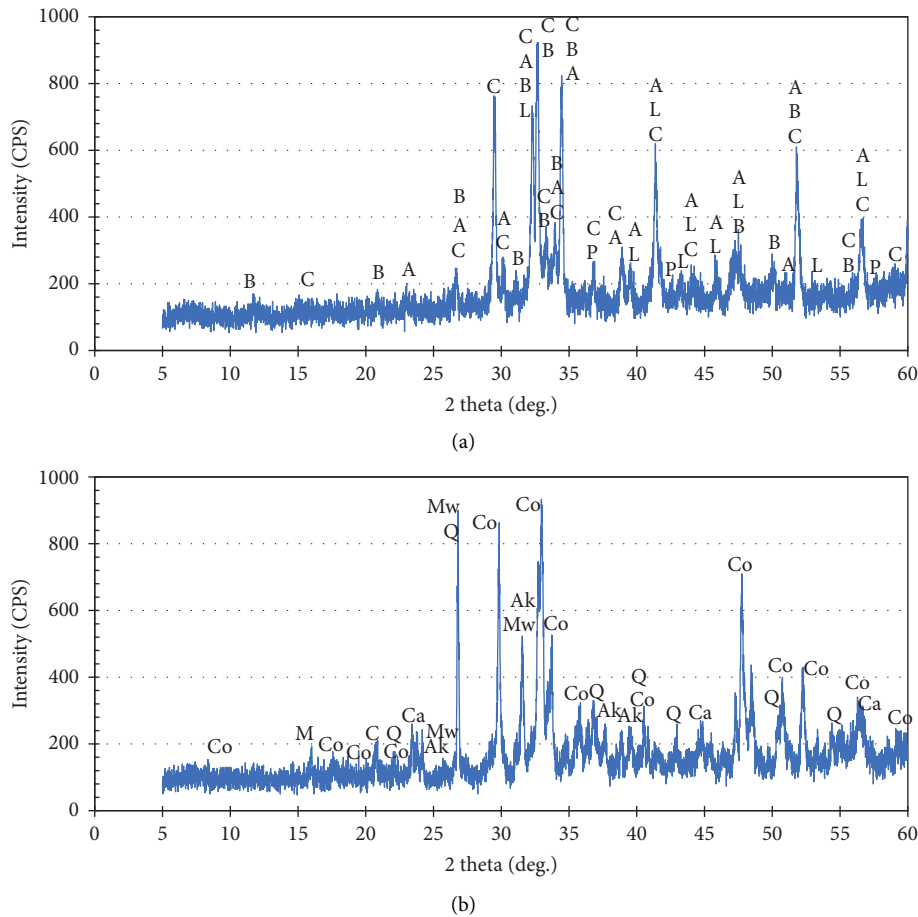| Oxides	CEM-I (this study)	Raw LFS (this study)	Raw LFS [54]	Raw LFS [8]
CaO (%)	60.4	47.4	48.4	30~60
SiO_2 (%)	29.4	29.4	15	2~35
Al_2O_3 (%)	2.6	2.6	14.3	4.1~35.9
Fe_2O_3 (%)	2.8	0.7	1.5	—
FeO (%)	—	—	—	0~15
MgO (%)	2	2.3	15.3	1~12.6
Na_2O (%)	1.5	1.6	0.4	0.06~0.07
K_2O (%)	0.7	0.1	0.4	0.01~0.02
TiO_2 (%)	0.6	0.9	0.2	0.2~0.9
MnO (%)	0.04	1.6	-	0~5

(a)

(b)

FIGURE 7: XRD patterns of (a) CEM-I and (b) LFS.

reduced with coarser SCM particles, it lowers the volume of hydration products [61].

The performance of sieved LFS is significantly better at an early age (7 days). This may be due to the nucleation effects in mortars [5]. At later ages, the unreacted LFS helps to fill the voids and form a denser mixture. Pozzolanic reaction products are more effective in filling pores. This filler effect can improve the transition zone and cement matrix property [62]. The water-cement ratio increases with SCM dosage. As a result, water-filled capillary space also increases, increasing the degree of hydration [61].

4.6.2. Influence of LFS Replacement. As shown in Figures 10(a) and 10(b), 7-days compressive strength of the control mortar is 35.6 MPa. For 5% raw LFS, the strength increased by 12% compared with the control, while 21.5% increase in strength for sieved LFS is achieved. The strength is comparable to the control (within ±10%) up to 10% replacement by raw LFS and 15% by sieved LFS. The secondary reaction between cement hydration by-products and the aluminosilicate compounds present in the LFS creates further bonding and improves the strength. Beyond these replacement levels, the strength decreases linearly, and a

TABLE 3: Mineralogical phases present in CEM-I and LFS with a chemical formula.

Symbol	Compound	Chemical formula
C	Alite/tricalcium silicate	$3CaO \cdot SiO_2$ (C_3S)
A	Tri calcium aluminate	$Ca_3Al_2O_6$ (C_3A)
B	Brownmillerite/tetracalcium aluminoferrite	$4CaO.Al_nFe_{2-n}O_3$ (C_4AF)
L	Larnite/dicalcium silicate	$\beta - Ca_2SiO_4$
P	Periclase	MgO
Co	Calcio-olivine	$\gamma - Ca_2SiO_4$
M	Magnetite	Fe_3O_4
Mw	Merwinite	$Ca_3Mg\,[SiO_4]_2$
Q	α-Quartz	SiO_2
Ca	Calcium-aluminium oxide	$CaAl_2O_4$
Ak	Akermanite	$Ca_2Mg\,[Si_2O_7]$

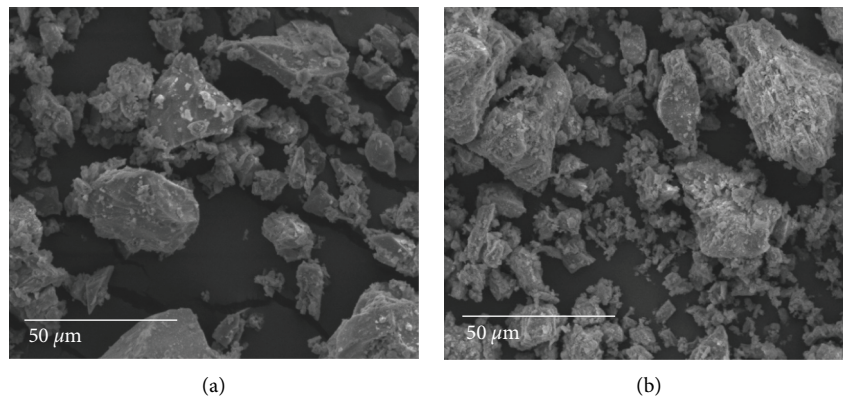(a)   (b)

FIGURE 8: Morphology of (a) CEM-I and (b) LFS obtained from SEM.

dramatic fall is observed for 50% LFS replacement. Wang [63] reports that reactivity of SCM reduces with the increase in replacement dosage.

As can be seen from Figure 10(a) (results of raw LFS), for 28 days curing, 5% raw LFS in mortar gives 5% higher compressive strength than that of the control mortar (43.7 MPa). Strength with 10% raw LFS replacement is similar to control mortar. For other replacement amount (i.e., 15%, 20%, 25%, and 50%), the strength reduces by 10.2%, 17.4%, 21.2%, and 57.4%, respectively. For the case of 56 days curing, 5% and 10% replacement with raw LFS gives 8.6% and 3.4% higher strength than the control mortar (48.2 MPa). The strength gain with SCM can be attributed to the fact that the reaction between silica (SiO_2) or alumina (Al_2O_3) and $Ca(OH)_2$ leads to form C-S-H gel. The dilution effect of SCM on compressive strength is found to be dominant after a specific dosage. Beyond this, for 15%, 20%, 25%, and 50% replacement, the strength reduces by 1.8%, 8.3%, 11.5%, and 56.5%, respectively.

As can be seen from Figure 10(b) (sieved LFS), for 28 days curing, compressive strength increases by 8.6% for 5% sieved LFS replacement and then decreases as the sieved LFS in mortars increases. Strengths are 5.9%, 10.2%, 12.7%, 62.8% lower (compared with control) for the case of 15%, 20%, 25%, and 50% cement replacement with sieved LFS. Although, 10% replacement gives identical compressive strength as of the control mortar. For the case of 56 days curing, compressive strengths of 5% and 10% sieved LFS
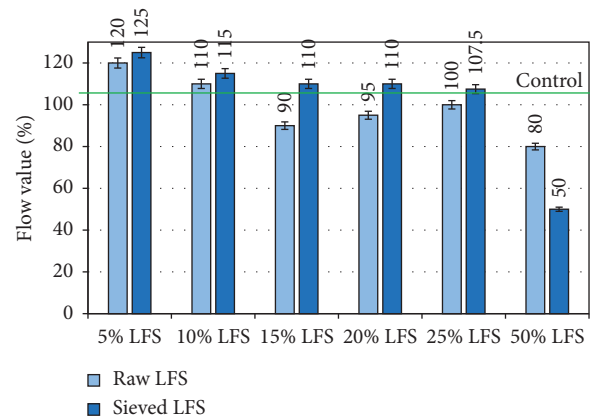

FIGURE 9: Flow value obtained for different LFS (raw and sieved) contents in mortar.

replacement in mortars are found to be higher (15.2% and 6.4%, respectively). Beyond that, the strength gradually reduces by 0.5%, 4.7%, 7.8%, and 44.7% for sieved LFS replacement of 15%, 20%, 25%, and 50%, respectively. Overall, sieved LFS shows better compressive strength than the raw material. With the increase of fineness, the hydration rate of C3S gets accelerated, resulting in strength increase [66].

An earlier study by Santamaria et al. [58] reports that 8%, 16%, 26%, and 46% strength loss can occur if of 10%, 20%, 30%, and 40% of cement in mortar is replaced by LFS.
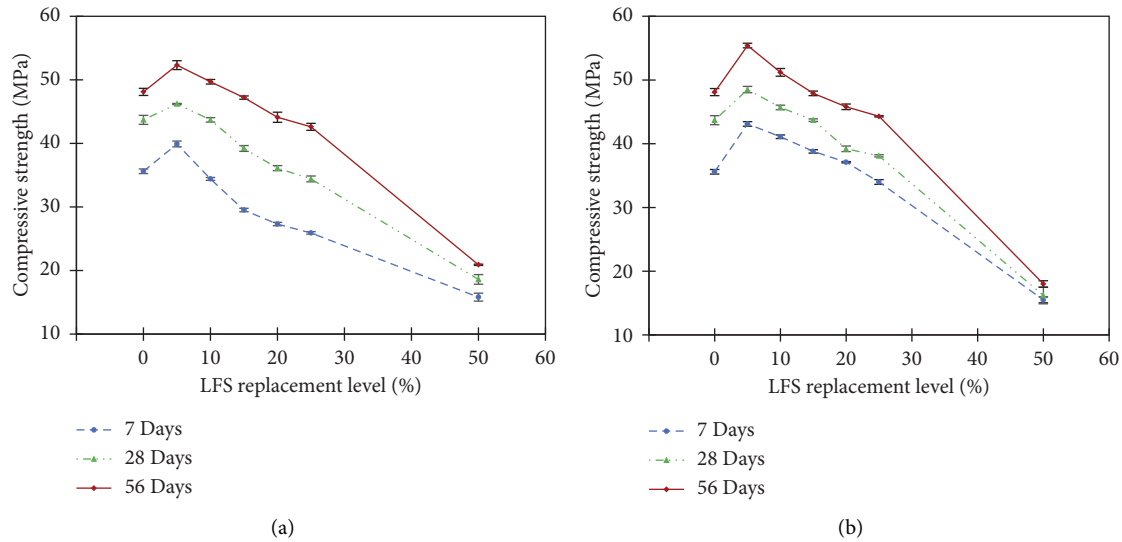
FIGURE 10: Relationship between compressive strength and LFS level in mortar: (a) mortar with raw LFS; (b) mortar with sieved LFS.

Another study reports that compressive strength reduces for mortars partially replaced (more than 20%) with LFS [42]. Previous studies recommend a different amount of LFS replacement, for example, [24]. Manso et al. [32] suggest up to 43% LFS to use in concrete, whereas Chang et al. [65] recommend up to 20% cement replacement with LFS to use in concrete. This study broadly suggests that up to 15% cement replacement with LFS would produce mortar of acceptable strength for regular construction.

4.6.3. Effect of Curing Time on Mortar Strength. The strengths of a few selected mortar samples with prolonged curing are shown in Figure 11, which presents relationships between compressive strength and curing time (7, 28, 56, 90, and 180 days) for raw LFS (Figure 11(a)) and for sieved LFS (Figure 11(b)). The strength of control mortar is compared with 25% and 50% LFS blended mortars of both types (raw and sieved).

The reason for above phenomenon may be attributed to hydration of cement. The cement hydration reaction starts immediately after adding water to cement. Even after replacing the cement with SCM, a reaction process initiates by which the mixture gets stiffened and attains its strength. The heat helps in faster hydration reaction and forms C-S-H gel rapidly. The pozzolanic effect also gets intensified at higher temperatures. However, in some cases, the 'crossover effect' at high temperature may cause reduction of strength [66]. Türkel and Alabas [67] report 65–70°C as the optimum temperature for accelerated curing. If the curing temperature crosses this limit for a more extended period, a drastic later age strength reduction may occur. This study, therefore, considered a limited period of high-temperature curing regime as per BS 3892 [68].

Results obtained for LFS blended 7 days HTAC mortars are compared with LFS blended 28 days NTC mortars in Figure 13. Figure 13(a) presents compressive strength as a function of raw LFS level and Figure 13(b) presents same for the sieved samples. It is evident from Figures 13(a) and 13(b) that by increasing the curing temperature, mortars can gain their strength much quicker than it would gain under standard or normal temperature curing. For both raw and sieved LFS blended mortars, strengths of 7 days' HTAC mortars at 5%, 10%, 15%, 20%, 25%, and 50% replacements are close (within 10%) to that of 28 days' NTC mortars. Mortars under accelerated curing were reported by Esen and Kurt [69] where cement was replaced partially by nanosilica, and by Islam [60] where cement was partially replaced by fly ash. They observed that compressive strength was increased by 5–11% when the curing temperature was accelerated. Erdem et al. [70] discuss that an accelerated curing system is incorporated in the prefabrication industry to reduce the cycle time of strength gain eventually allowing for cost-saving.

For 25% LFS replacement, an increase in compressive strength can be noticed at 90 days curing, which is true for both raw (Figure 11(a)) and sieved LFS blends (Figure 11(b)). However, 50% LFS (both raw and sieved) replacement gives no promising results even for an extended curing period, probably due to greater loss of reactivity with increased SCM [63]. For both percentages, strength improvement between 90 and 180 days is insignificant, again, true for both raw and sieved LFS blends (Figures 11(a) and 11(b)). For sieved LFS at 90 days curing, strength of 25% LFS blended mortar is within the 10% of control mortar (Figure 11(b)): compressive strength value of 45 MPa at this age (90 days) would be promising for any structural use, especially for foundation work where continuous hydration by groundwater is possible. From Figures 11(a) and 11(b), the similar strength of raw and sieved LFS at 90 days indicates that all materials can eventually react with time regardless of size.
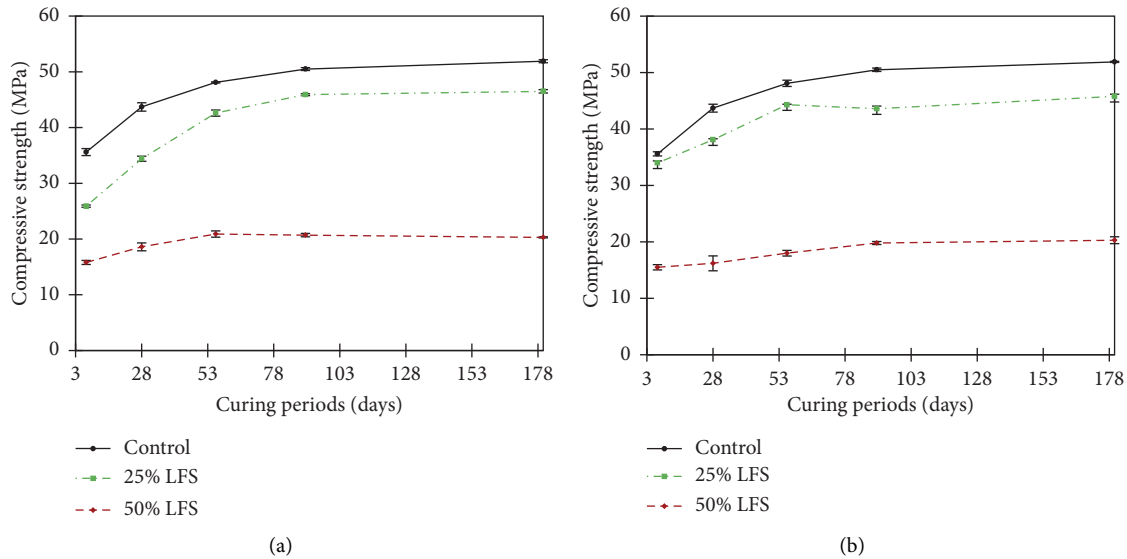
FIGURE 11: Relationship between compressive strength of mortar and curing period: (a) mortars with raw LFS; (b) mortars with sieved LFS.
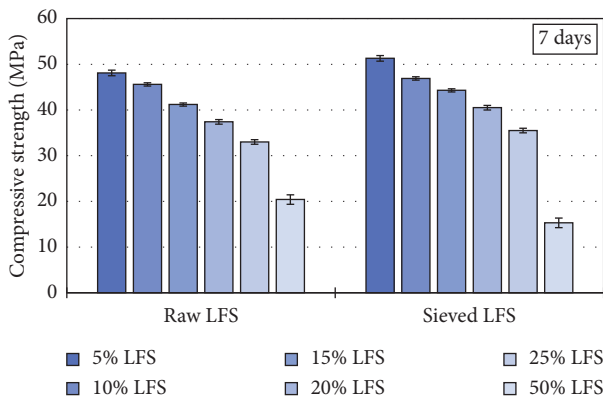

FIGURE 12: Compressive strength (nominal 7 days) of LFS-blended HTAC mortars (7 days include 46 hours high-temperature curing at 50±1°C).

4.7. Mortar Strength for High-Temperature Accelerated Curing (HTAC).

The effect of high-temperature accelerated curing (HTAC) on mortar strength is discussed here based on Figure 12. Limited period high-temperature (46 hours at 50±1°C) curing (overall about 7 days curing) shows a significant influence on the compressive strength of LFS blended mortars (raw and sieved) of various replacement percentages (5, 10, 15, 20, 25, and 50%). Results for LFS blended HTAC (both raw and sieved) mortars indicate that 5–20% cement replacement with LFS gives higher strength (above 37 MPa). These values are close to 28 days' strength (36.1 MPa) of mortars in normal temperature curing (NTC). As can also be seen from Figure 12, under HTAC, sieved LFS blended mortar performs better (which was true for sieved LFS mortars under NTC; Figure 10(b)).

4.8. Practical Implications.

Apart from producing eco-friendly mortar (which is a default benefit), use of LFS as a partial replacement to cement may reduce the construction cost. Figure 14 (considering 5% more or less) gives an approximate estimation of the cost savings–standard market prices of the constituent ingredients are considered. In Bangladesh, the cost of 1 tonne LFS is $30 (USD), according to a steel mill's contract with a known company (personal communication). That means 50 kgs of LFS would cost approximately $1.5. An additional $0.5 can be considered (from experience) for other costs, such as transportation, handling, and storage. Then the total cost would be $2. On the other hand, 50 kgs (1 bag) of Portland cement in Bangladesh costs approximately $6 (3 times higher than the cost of LFS). Therefore, partial replacement of about 15% (as can be derived from this study) of cement by LFS may substantially reduce the cost, and an eventual reduction of cement use by 15%. For the case where strength is reduced by 10–20% when cement is replaced by LFS for up to 25% replacement, the compromised strength of the blended cement could still be used for non-structural work, and production of cement can be reduced by 25% as well. With a 15% blending of LFS in cement, the overall cost-saving will probably be 11% (Figure 14). This saving will increase up to 18.5% for 25% cement replacement with LFS.

In addition, the environmental benefit of using LFS as SCM can also be quantified, indirectly though. Recent and previous reports mention that appx. 90% of CO_2 can be emitted during cement production [71, 72], i.e., 900 kg of CO_2 is being released when 1 tonne cement is produced. A simple calculation results as shown in Figure 15 suggests that 20% of LFS use will cause 72% of CO_2 generation which would otherwise cause a 90% CO_2 generation if only cement
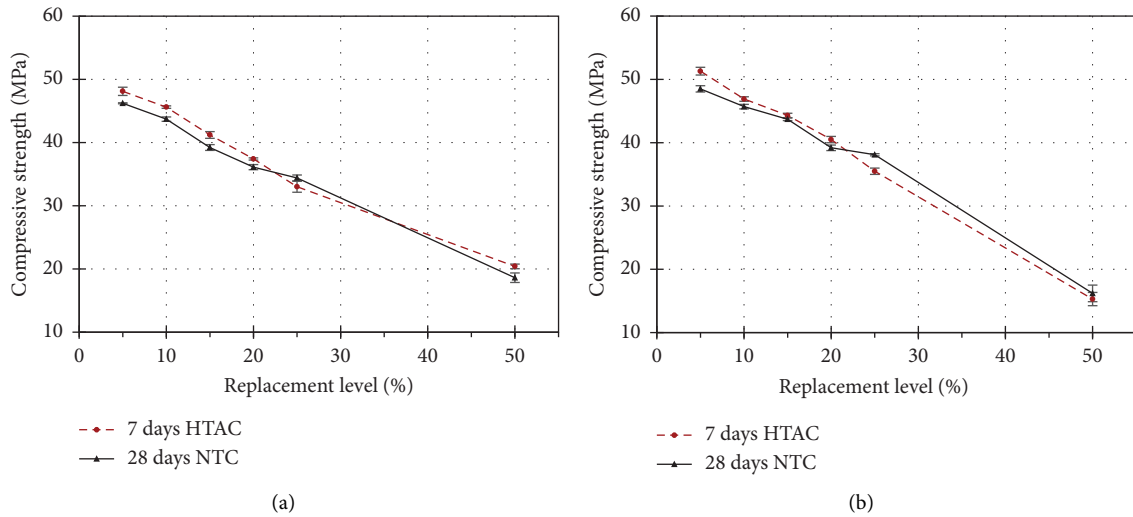
FIGURE 13: Strength comparison between 7 days HTAC mortars and 28 days NTC mortars. (a) Raw LFS-blended mortars; (b) Sieved LFS-blended mortars.
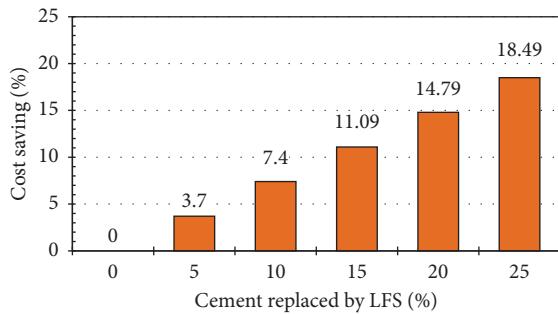

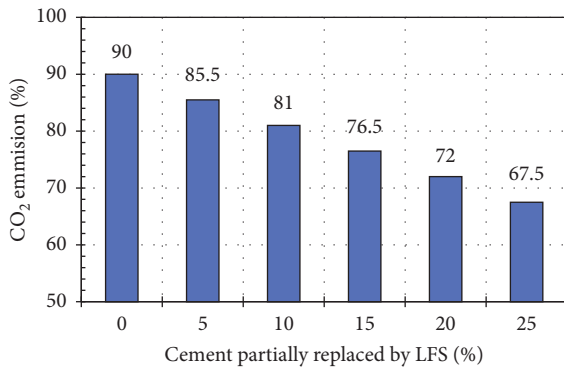FIGURE 14: Probable economic benefit of partial cement replacement by LFS.

FIGURE 15: Probable reduction in CO_2 generation due to LFS use.

was used (any emission attributed to LFS production is ignored here). This is in line with the published report of Campos et al. [73] that states a yearly reduction of 100 thousand tonnes of CO_2 when cement in concrete is reduced by 5 kg per cubic metre.

Further evidences of environmental benefit of using LFS in mortar (or concrete in a broader sense) can be inferred from the study of Perez-garcia et al. [74]. They

conducted a leachate test on Portland cement and LFS (30% substitution) for selected chemical elements and reported that leaching potential was less in LFS mixed concrete compared with control concrete. They have further reported that presence of chromium (Cr) was significant in control concrete. For the case of LFS, the level of Cr was within the Code of Federal Regulation limit (5 mg/L). It was concluded that LFS replaced with cement may dilute the cement matrix paste and absorb this element, hence, no additional environmental hazard would take place. Other leachates were found like the conventional concrete. Their report hints that it is wise to manage LFS slag by encapsulating it into cementitious media rather than depositing it as a landfill. Direct deposition in landfill may leach the harmful chemical compounds/heavy metals to the environment [75].

5. Conclusion

In this study, a locally available LFS was first characterized for its chemical and physical properties. Then, the LFS was incorporated in mortar as a partial replacement of cement. Two forms of the LFS were used: raw (as-received) and sieved (#200 sieve). The compressive strengths of mortars, prepared with various LFS percentages (0, 5%, 10%, 15%, 20%, 25%, 50%) of raw and sieved LFS and cured under normal temperature (NTC) for 7, 28, and 56 days, were obtained and reported. Selected samples were cured for 90 and 180 days. Additionally, raw and sieved LFS blended mortars under high-temperature accelerated curing (HTAC) were tested (at 7 days) and reported in this study. The key conclusions arisen from this study on raw and sieved LFS blended mortars, are as follows:

(1) Chemical composition of LFS gives similar oxides to that of CEM-I. The amount of CaO, SiO_2, MgO, and Al_2O_3 in raw LFS collectively cover more than 92% of the total mass.

(2) The mineralogical phases present in the raw LFS are calcio-olivine, akermanite, α-quartz (SiO_2), merwinite, magnetite, and calcium-aluminium oxide.

(3) Morphology of LFS is a whitish dusty surface. The grains are found with sharp edges. The surface contains significant cracks with roughness.

(4) The performance of LFS in mortar is improved using smaller size by sieving. In general, 5–15% cement replacement with LFS (raw and sieved) provides better or comparable performance than/to control mortars. Reasonable compressive strength is found with 15% LFS replacement.

(5) Compressive strength of the raw and sieved LFS blended mortars generally increases with curing period up to 90 days. Further curing beyond that offers very marginal strength.

(6) Seven days compressive strengths of raw and sieved LFS blended HTAC mortars were found to be well comparable to the strengths of 28 days NTC mortars.

This study endorses that LFS considered in this study can be an excellent SCM, preferably up to 15% cement substitution. However, further investigation is indispensable to explore the mechanical and durability properties of hardened concrete prepared with similar LFS as SCM. This is being considered by the authors and will be reported in a forthcoming paper.

Data Availability

Some or all data, models, or codes that support the findings of this study are available from the corresponding author upon reasonable request.

Conflicts of Interest

The authors declare that they have no conflicts of interest.

Authors' Contributions

Iffat Sultana was responsible for conceptualization; methodology; experimental work; analysis; and original draft preparation. G. M. Sadiqul Islam was involved in conceptualization; methodology; material arrangement; editing; and supervision.

Acknowledgments

References

[1] J. Lehne and F. Preston, *Making Concrete Change; Innovation in Low-carbon Cement and Concrete*, Chatham House Rep, London, UK, pp. 1–122, 2018.

[2] IEA, *Cement*, IEA, Paris, 2020.

[3] BCMA, *Overview of Cement Industry*, Dhaka, Bangladesh, 2021.

[4] I. Sultana and G. M. S. Islam, *Applicability of Treated Industrial Wastewater in concrete Construction*, pp. 12-13, Southern University Bangladesh, Chittagong, 2018.

[5] G. S. Islam, M. H. Rahman, and N. Kazi, "Waste glass powder as partial replacement of cement for sustainable concrete practice," *International Journal of Sustainable Built Environment*, vol. 6, no. 1, pp. 37–44, 2017.

[6] A. Naceri and M. C. Hamina, "Use of waste brick as a partial replacement of cement in mortar," *Waste Management*, vol. 29, no. 8, pp. 2378–2384, 2009.

[7] H. Toutanji and T. El-Korchi, "The influence of silica fume on the compressive," *Cement and Concrete Research*, vol. 25, pp. 1591–1602, 1995.

[8] I. Z. Yildirim and M. Prezzi, "Chemical, mineralogical, and morphological properties of steel slag," *Advances in Civil Engineering*, vol. 2011, pp. 1–13, 2011.

[9] A. A. Phul, M. J. Memon, S. N. R. Shah, and A. R. Sandhu, "GGBS and fly ash effects on compressive strength by partial replacement of cement concrete," *Civil Engineering J.*vol. 5, no. 4, pp. 913–921, 2019.

[10] R. Roy and V. Sairam, "Effect of Silica Fume and Foundry waste sand on strength characteristics of Geogrid and Ferro cement panel," *Materials Today Proceedings*, vol. 7, pp. 362–372, 2019.

[11] B. Xu and Y. Yi, "Soft clay stabilization using ladle slag-ground granulated blastfurnace slag blend," *Applied Clay Science*, vol. 178, Article ID 105136, 2019.

[12] P. Saloni, Y. Y. Lim, Y. Y. Lim, T. M. Pham, and P. Negi, "Performance enhancement of rubberised-alkali-activated-concrete utilising ultra-fine slag and fly ash," *Cleaner Materials*, vol. 4, Article ID 100080, 2022.

[13] G. M. S. Islam and A. Akter, "Rice husk ash as a sustainable construction material for Bangladesh," in *1st International Conference on Advances in Civil Engineering (ICACE 2012)* Department of Civil Engineering, Chittagong University of Engineering & Technology (CUET), Chittagong, Bangladesh, 2012.

[14] K. H. Mo, U. J. Alengaram, M. Z. Jumaat, S. P. Yap, and S. C. Lee, "Green concrete partially comprised of farming waste residues: a review," *Journal of Cleaner Production*, vol. 117, pp. 122–138, 2016.

[15] K. Perumal, A. Kumar, N. Lingeshwaran, and S. Susmitha, "Experimental studies on flexural behaviour of self compact concrete beam," *Materials Today: Proceedings. Elsevier*, vol. 33, no. 1, pp. 129–135, 2020.

[16] J. Payá, J. Monzó, M. V. Borrachero, L. Soriano, J. L. Akasaki, and M. M. Tashima, "New inorganic binders containing ashes from agricultural wastes," *Sustainable and Nonconventional Construction Materials Using Inorganic Bonded Fiber Composites. Elsevier, Chapter 5*, pp. 127–164, 2017.

[17] G. Martínez-Barrera, C. E. Barrera-Díaz, E. Cuevas-Yañez et al., "Waste cellulose from tetra pak packages as reinforcement of cement concrete," *Advances in Materials Science and Engineering, Special Issue, Green Composite Materials*, vol. 2015, 6 pages, 2015.

[18] D. Barua, "Effectiveness of use of rice husk ash as partial replacement of cement in concrete," in *Proceedings of the 4th International Conference on Civil Engineering for Sustainable Development*, KUET, Khulna, Bangladesh, 2018.

[19] M. A. Hasan, "A Study on the Use of rice Husk Ash (RHA) as Partial Replacement of Cement in concrete," *Engineering Heritage Journal*, vol. 3, no. 1, pp. 01–04, 2020.

[20] G. M. S. Islam, M. M. Islam, A. Akter, and M. S. Islam, "Green construction materials – Bangladesh perspective," in *Proceedings of the International Conference on Mechanical Engineering and Renewable Energy (ICMERE2011)*, Department of Mechanical Engineering, CUET, Bangladesh., Chittagong, 2011.

[21] S. I. Ahmad, "Mechanical and Durability Properties of Induction-Furnace-Slag-Incorporated Recycled 2018," *Journal of Building Engineering*, vol. 61, Article ID 105301, 2018.

[22] M. Mahoutian and Y. Shao, "Low temperature synthesis of cement from ladle slag and fly ash," *Journal of Sustainable Cement-Based Materials*, vol. 5, no. 4, pp. 247–258, 2016.

[23] Y. Jiang, T. C. Ling, C. Shi, and S. Y. Pan, "Characteristics of steel slags and their use in cement and concrete—a review," *Resources, Conservation and Recycling*, vol. 136, pp. 187–197, 2018.

[24] J. M. Manso, M. Losañez, J. A. Polanco, and J. J. Gonzalez, "Ladle furnace slag in construction," *Journal of Materials in Civil Engineering*, vol. 17, no. 5, pp. 513–518, 2005.

[25] G. S. Islam, S. Akter, and T. B. Reza, "Sustainable high-performance, self-compacting concrete using ladle slag," *Cleaner Engineering and Technology*, vol. 7, Article ID 100439, 2022.

[26] J. Setién, D. Hernández, and J. J. González, "Characterization of ladle furnace basic slag for use as a construction material," *Construction and Building Materials*, vol. 23, no. 5, pp. 1788–1794, 2009.

[27] J. M. Manso, V. Ortega-López, J. A. Polanco, and J. Setién, "The use of ladle furnace slag in soil stabilization," *Construction and Building Materials*, vol. 40, pp. 126–134, 2013.

[28] J. M. Montenegro, D. Ph, J. Cañizal, D. Ph, J. Setién, and D. Ph, "Ladle Furnace Slag in the Construction of Embankments: Expansive Behavior Ladle Furnace Slag in the Construction of Embankments," *Expansive Behavior, Journal of Materials in Civil Engineering*, vol. 25, no. 8, 2013.

[29] M. Skaf, V. Ortega-López, J. A. Fuente-Alonso, A. Santamaría, and J. M. Manso, "Ladle furnace slag in asphalt mixes," *Construction and Building Materials*, vol. 122, pp. 488–495, 2016.

[30] C. Shi and J. Qian, "High performance cementing materials from industrial slags — a review," *Resources, Conservation and Recycling*, vol. 29, no. 3, pp. 195–207, 2000.

[31] C. Shi, "Characteristics and cementitious properties of ladle slag fines from steel production," *Cement and Concrete Research*, vol. 32, no. 3, pp. 459–462, 2002.

[32] J. M. Manso, Á. Rodriguez, Á. Aragón, and J. J. Gonzalez, "The durability of masonry mortars made with ladle furnace slag," *Construction and Building Materials*, vol. 25, no. 8, pp. 3508–3519, 2011.

[33] E. Adesanya, H. Sreenivasan, A. M. Kantola et al., "Ladle slag cement – characterization of hydration and conversion," *Construction and Building Materials*, vol. 193, pp. 128–134, 2018.

[34] L. Kriskova, Y. Pontikes, Ö. Cizer et al., "Effect of mechanical activation on the hydraulic properties of stainless steel slags," *Cement and Concrete Research*, vol. 42, no. 6, pp. 778–788, 2012.

[35] C. Shi and S. Hu, "Cementitious properties of ladle slag fines under autoclave curing conditions," *Cement and Concrete Research*, vol. 33, no. 11, pp. 1851–1856, 2003.

[36] Y.-N. Sheen, D.-H. Le, and T.-H. Sun, "Innovative usages of stainless steel slags in developing self-compacting concrete," *Construction and Building Materials*, vol. 101, pp. 268–276, 2015.

[37] M. Salman, Ö. Cizer, Y. Pontikes et al., "Cementitious binders from activated stainless steel refining slag and the effect of alkali solutions," *Journal of Hazardous Materials*, vol. 286, pp. 211–219, 2015.

[38] S. Choi, J.-M. Kim, D. Han, and J.-H. Kim, "Hydration properties of ladle furnace slag powder rapidly cooled by air," *Construction and Building Materials*, vol. 113, pp. 682–690, 2016.

[39] A. Natali Murri, W. D. A. Rickard, M. C. Bignozzi, and A. Van Riessen, "High temperature behaviour of ambient cured alkali-activated materials based on ladle slag," *Cement and Concrete Research*, vol. 43, pp. 51–61, 2013.

[40] O. Najm, H. El-Hassan, and A. El-Dieb, "Ladle slag characteristics and use in mortar and concrete: a comprehensive review," *Journal of Cleaner Production*, vol. 288, Article ID 125584, 2021.

[41] A. Bougara, C. Lynsdale, and K. Ezziane, "Activation of Algerian slag in mortars," *Construction and Building Materials*, vol. 23, no. 1, pp. 542–547, 2009.

[42] I. Papayianni and E. Anastasiou, "Effect of granulometry on cementitious properties of ladle furnace slag," *Cement and Concrete Composites*, vol. 34, no. 3, pp. 400–407, 2012.

[43] M. R. Irshidat and N. Al-Nuaimi, "Industrial waste utilization of carbon dust in sustainable cementitious composites production," *Materials*, vol. 13, no. 15, p. 3295, 2020.

[44] A. Rodriguez, I. Santamaría-Vicario, V. Calderón, C. Junco, and J. García-Cuadrado, "Study of the expansion of cement mortars manufactured with Ladle Furnace Slag (LFS)," *Materiales de Construcción*, vol. 69, no. 334, p. 183, 2019.

[45] R. Meier, J. Anderson, and S. Verryn, "Industrial X-ray diffraction analysis of building materials," *Reviews in Mineralogy and Geochemistry*, vol. 74, no. 1, pp. 147–165, 2012.

[46] J. P. R. De Villiers and L. Lu, "XRD analysis and evaluation of iron ores and sinters," *Iron Ore Mineral. Process. Environ. Sustain.* vol. 85, p. 100, 2015.

[47] Z. He, C. Qian, Y. Zhang, F. Zhao, and Y. Hu, "Nanoindentation characteristics of cement with different mineral admixtures," *Science China Technological Sciences*, vol. 56, no. 5, pp. 1119–1123, 2013.

[48] M. A. Uddin, M. Jameel, H. R. Sobuz, N. M. S. Hasan, M. S. Islam, and K. M. Amanat, "The effect of curing time on compressive strength of composite cement concrete," *Applied Mechanics and Materials*, vol. 204-208, pp. 4105–4109, 2012.

[49] N. Yong-Sing, L. Yun-Ming, H. Cheng-Yong et al., "Evaluation of flexural properties and characterisation of 10-mm thin geopolymer based on fly ash and ladle furnace slag," *Journal of Materials Research and Technology*, vol. 15, pp. 163–176, 2021.

[50] M. J. McCarthy, G. M. S. Islam, L. J. Csetenyi, and M. R. Jones, "Refining the foam index test for use with air-entrained fly ash concrete," *Magazine of Concrete Research*, vol. 64, no. 11, pp. 967–978, 2012.

[51] H. T. Türker, M. Balçikanli, I. H. Durmuş, E. Özbay, and M. Erdemir, "Microstructural alteration of alkali activated slag mortars depend on exposed high temperature level," *Construction and Building Materials*, vol. 104, pp. 169–180, 2016.

[52] M. Salman, Ö. Cizer, Y. Pontikes, L. Vandewalle, B. Blanpain, and K. Van Balen, "Effect of curing temperatures on the alkali activation of crystalline continuous casting stainless steel slag," *Construction and Building Materials*, vol. 71, pp. 308–316, 2014.

[53] C. Shi, "Steel slag—its production, processing, characteristics, and cementitious properties," *Journal of Materials in Civil Engineering*, vol. 16, no. 3, pp. 230–236, 2004.

[54] A. Radenović, J. Malina, and T. Sofilić, "Characterization of ladle furnace slag from carbon steel production as a potential adsorbent," *Advances in Materials Science and Engineering*, vol. 20136 pages, 2013.

[55] G. Kürklü, "The effect of high temperature on the design of blast furnace slag and coarse fly ash-based geopolymer mortar," *Composites Part B: Engineering*, vol. 92, pp. 9–18, 2016.

[56] B. Balakrishnan, A. S. M. A. Awal, A. H. B. Abdullah, and M. Z. Hossain, "Flow properties and strength behaviour of masonry mortar incorporating high volume fly ash," *International Journal of GEOMATE*, vol. 12, no. 31, pp. 121–126, 2017.

[57] M. J. McCarthy, G. M. S. Islam, L. J. Csetenyi, and M. R. Jones, *Evaluating test methods for rapidly assessing flyaAsh reactivity for use in concrete*, World of Coal Ash Conference, Lexington, Kentucky, USA, 2013.

[58] A. Santamaria, V. Ortega-Lopez, M. Skaf et al., "Ladle furnace slag as cement replacement in mortar mixes," *Sustain. Constr. Mater. Technol.*vol. 1, 2019.

[59] A. K. Zykova, P. V. Pantyukhov, N. N. Kolesnikova, A. A. Popov, and A. A. Olkhov, "Influence of particle size on water absorption capacity and mechanical properties of polyethylene-wood flour composites," *AIP Conference Proceedings*, vol. 1683, 2015.

[60] G. M. S. Islam, *Evaluating Reactivity and Sorptivity of Fly Ash for Use in concrete Construction*, University of Dundee, Dundee, Scotland, 2012.

[61] N. Neithalath, "Quantifying the effects of hydration enhancement and dilution in cement pastes containing coarse glass powder," *Journal of Advanced Concrete Technology*, vol. 6, no. 3, pp. 397–408, 2008.

[62] M. Singh, A. Srivastava, and D. Bhunia, "An investigation on effect of partial replacement of cement by waste marble slurry," *Construction and Building Materials*, vol. 134, pp. 471–488, 2017.

[63] X. Y. Wang, "Effect of fly ash on properties evolution of cement based materials," *Construction and Building Materials*, vol. 69, pp. 32–40, 2014.

[64] V. L. Bonavetti, V. F. Rahhal, and E. F. Irassar, "Studies on the carboaluminate formation in limestone filler-blended cements," *Cement and Concrete Research*, vol. 31, no. 6, pp. 853–859, 2001.

[65] S. Y. Chang, S. C. Chen, C. Tu, and Y. W. Tseng, "Ladle furnace slag as a sustainable binder for masonry mortars," *Key Engineering Materials*, vol. 801, pp. 385–390, 2019.

[66] J. Payá, J. Monzó, E. Peris-Mora, M. V. Borrachero, R. Tercero, and C. Pinillos, "Early-strength development of portland cement mortars containing air classified fly ashes," *Cement and Concrete Research*, vol. 25, no. 2, pp. 449–456, 1995.

[67] S. Türkel and V. Alabas, "The effect of excessive steam curing on Portland composite cement concrete," *Cement and Concrete Research*, vol. 35, no. 2, pp. 405–411, 2005.

[68] A. F. Abdalqader, F. Jin, and A. Al-Tabbaa, "Development of greener alkali-activated cement: utilisation of sodium carbonate for activating slag and fly ash mixtures," *Journal of Cleaner Production*, vol. 113, pp. 66–75, 2016.

[69] Y. Esen and A. Kurt, "Effect of high temperature in concrete for different mineral additives and rates," *KSCE Journal of Civil Engineering*, vol. 22, no. 4, pp. 1288–1294, 2018.

[70] T. K. Erdem, L. Turanli, and T. Y. Erdogan, "Setting time: an important criterion to determine the length of the delay period before steam curing of concrete," *Cement and Concrete Research*, vol. 33, no. 5, pp. 741–745, 2003.

[71] S. C. Bostanci, "Use of waste marble dust and recycled glass for sustainable concrete production," *Journal of Cleaner Production*, vol. 251, Article ID 119785, 2020.

[72] M. Nisbet and M. G. Van Geem, "Environmental life cycle inventory of Portland cement and concrete," *World Cem*, vol. 28, 1997.

[73] H. F. Campos, N. S. Klein, and J. Marques Filho, "Proposed mix design method for sustainable high-strength concrete using particle packing optimization," *Journal of Cleaner Production*, vol. 265, Article ID 121907, 2020.

[74] F. Perez-garcia, A. Gonzalez-herrera, M. Jos, and M. D. Rubio-cintas, "Concrete: Mechanical , Physical and Environmental Properties," *Cement and Concrete Research*, vol. 27, no. 12, pp. 1817–1823, 2019.

[75] S. S. Varanasi, V. M. R. More, M. B. V. Rao, S. R. Alli, A. K. Tangudu, and D. Santanu, "Recycling ladle furnace slag as flux in steelmaking: a review," *J. Sustain. Metall.*vol. 5, no. 4, pp. 449–462, 2019.